Title 論文題目	Xanthine oxidoreductase-mediated injury is amplified by upregulated AMP deaminase in type 2 diabetic rat hearts under the condition of pressure overload. (2型糖尿病ラットにおいて、キサンチン酸化還元酵素による心機能障害はAMPデアミナーゼ活性亢進により圧負荷下で増幅される)
Author(s) 著者	井垣, 勇祐
Degree number 学位記番号	甲第3138号
Degree name 学位の種別	博士(医学)
Issue Date 学位取得年月日	2021-03-31
Original Article 原著論文	J Mol Cell Cardiol. 2021 May;154:21-31
Doc URL	
DOI	10.1016/j.yjmcc.2021.01.002
Resource Version	Publisher Version

Journal of Molecular and Cellular Cardiology 154 (2021) 21–31

Contents lists available at ScienceDirect

Journal of Molecular and Cellular Cardiology

journal homepage: www.elsevier.com/locate/yjmcc

Xanthine oxidoreductase-mediated injury is amplified by upregulated AMP deaminase in type 2 diabetic rat hearts under the condition of pressure overload

Yusuke Igaki [a,1], Masaya Tanno [a,1], Tatsuya Sato [b], Hidemichi Kouzu [a], Toshifumi Ogawa [a], Arata Osanami [a], Toshiyuki Yano [a], Atsushi Kuno [c], Takayuki Miki [a], Takashi Nakamura [d], Tetsuji Miura [a,*]

[a] Department of Cardiovascular, Renal and Metabolic Medicine, Sapporo Medical University School of Medicine, Sapporo, Japan
[b] Department of Cellular Physiology and Signal Transduction, Sapporo Medical University School of Medicine, Sapporo, Japan
[c] Department of Pharmacology, Sapporo Medical University School of Medicine, Sapporo, Japan.
[d] Pharmaceutical Research Laboratories, Sanwa Kagaku Kenkyusho, Mie, Japan

ARTICLE INFO

Keywords:
AMP deaminase
Xanthine oxidoreductase
Diabetic cardiomyopathy
Heart failure
Mitochondria

ABSTRACT

Background: We previously reported that upregulated AMP deaminase (AMPD) contributes to diastolic ventricular dysfunction via depletion of the adenine nucleotide pool in a rat model of type 2 diabetes (T2DM), Otsuka Long-Evans-Tokushima Fatty rats (OLETF). Meanwhile, AMPD promotes the formation of substrates of xanthine oxidoreductase (XOR), which produces ROS as a byproduct. Here, we tested the hypothesis that a functional link between upregulated AMPD and XOR is involved in ventricular dysfunction in T2DM rats.

Methods and results: Pressure-volume loop analysis revealed that pressure overloading by phenylephrine infusion induced severer left ventricular diastolic dysfunction (tau: 14.7 ± 0.8 vs 12.5 ± 0.7 msec, left ventricular end-diastolic pressure: 18.3 ± 1.5 vs 12.2 ± 1.3 mmHg, $p < 0.05$) and ventricular-arterial uncoupling in OLETF than in LETO, non-diabetic rats, though the baseline parameters were comparable in the two groups. While the pressure overload did not affect AMPD activity, it increased XOR activity both in OLETF and LETO, with OLETF showing significantly higher XOR activity than that in LETO (347.2 ± 17.9 vs 243.2 ± 6.1 μg/min/mg). Under the condition of pressure overload, myocardial ATP level was lower, and levels of xanthine and uric acid were higher in OLETF than in LETO. Addition of exogenous inosine, a product of AMP deamination, to the heart homogenates augmented XOR activity. OLETF showed 68% higher tissue ROS levels and 47% reduction in mitochondrial state 3 respiration compared with those in LETO. Overexpression of AMPD3 in H9c2 cells elevated levels of hypoxanthine and ROS and reduced the level of ATP. Inhibition of XOR suppressed the production of tissue ROS and mitochondrial dysfunction and improved ventricular function under the condition of pressure overload in OLETF.

Conclusions: The results suggest that increases in the activity of XOR and the formation of XOR substrates by upregulated AMPD contribute to ROS-mediated diastolic ventricular dysfunction at the time of increased cardiac workload in diabetic hearts.

1. Introduction

Diabetic cardiomyopathy is defined as cardiac dysfunction encompassing structural, functional and metabolic changes in the absence of coronary artery disease and hypertension [1,2]. A large population study revealed that the risk of hospitalization for heart failure in patients with type 2 diabetes was higher than that in non-diabetic subjects despite good control of other cardiovascular risk factors, while the increase in risk of myocardial infarction was negligible in those patients [3]. It has been reported that diastolic dysfunction precedes systolic

* Corresponding author at: Department of Cardiovascular, Renal and Metabolic Medicine, Sapporo Medical University School of Medicine, S1 W16, Chuo-ku, Sapporo 060-8543, Japan.
E-mail address: miura@sapmed.ac.jp (T. Miura).
[1] Yusuke Igaki and Masaya Tanno contributed equally to this work.

https://doi.org/10.1016/j.yjmcc.2021.01.002
Received 3 October 2020; Received in revised form 9 January 2021; Accepted 26 January 2021
Available online 4 February 2021

dysfunction in patients with diabetic cardiomyopathy [1] and diastolic dysfunction appears to predict cardiovascular mortality in type 2 diabetic patients, even in those without clinically manifest heart failure at rest [4]. Thus, treatment for diastolic dysfunction in diabetic patients would be of clinical importance, though no specific therapy is currently available for this disorder.

We recently reported that upregulation of AMP deaminase (AMPD) activity by reduced micro RNA (miR)-301b is one of the mechanisms underlying augmentation of diastolic dysfunction at the time of pressure overload in diabetic hearts [5,6]. AMPD activity was 2.5-fold higher in Otsuka Long-Evans-Tokushima fatty rats (OLETF), an established model of type 2 diabetes (T2DM) [5,6], than in LETO, non-diabetic control rats, and the upregulated AMPD activity was associated with an increase in the level of IMP and decreases in the levels of adenine nucleotide pool and ATP during ventricular pressure overloading [5]. Overexpression of flag-AMPD3, an exclusively dominant isoform in rats, resulted in reduction of ATP level in cardiomyocytes, indicating a causal relationship between increased AMPD activity and ATP depletion [6]. However, roles of increased IMP and inosine nucleosides by AMPD upregulation in diabetic cardiomyopathy have not been examined.

In the present study, we hypothesized that upregulated AMPD augments the pathological role of xanthine oxidoreductase (XOR), via increases in both XOR activity and formation of its substrates, in diabetic cardiomyopathy. The rationale for the hypothesis is three-fold. First, while XOR is synthesized in its constitutively active dehydrogenase form, it can be converted through sulfhydryl group oxidation or limited proteolysis to xanthine oxidase, a form that produces cytotoxic reactive oxygen species (ROS) [7,8]. Experimental studies using animal heart failure models demonstrated that administration of XOR inhibitors improved mechano-energetic coupling and left ventricular (LV) function, attenuated LV remodeling and promoted survival [9–12]. Notably, the magnitude of functional improvement with XOR inhibitors depends on the initial level of XOR activity [10], indicating that XOR inhibitors would be particularly effective in hearts with high XOR activity. Furthermore, some observational studies and meta-analyses showed that elevated serum uric acid level is an independent predictor of poor cardiac function and high mortality in patients with heart failure [13,14]. Second, our previous study showed that upregulated activity of AMPD in type 2 diabetic hearts results in elevation of the levels of IMP, inosine and xanthine, substrates of XOR, in the LV myocardium under the condition of pressure overload [5]. Third, increase in XOR activity under diabetic conditions has been reported in non-cardiac tissues [15–18]. We tested our hypothesis by using OLETF as a model of T2DM as in previous studies [5,6,19,20] since it has been shown that OLETF have many similarities to T2DM patients in terms of metabolic and cardiovascular phenotypes [1,5,21,22,23].

2. Methods

The methods used in this study are described in detail in Electronic Supplementary Material, Supplementary Methods. This study was conducted in strict accordance with the Guide for the Care and Use of Laboratory Animals published by National Research Council of the National Academies, USA (2011) and was approved by the Animal Use Committee of Sapporo Medical University.

2.1. Animal models

We used male OLETF and their non-diabetic controls, Long-Evans-Tokushima Fatty rats (LETO), at the age of 29–35 weeks in this study. The rats were maintained in a 14 h/10 h light–dark cycle temperature-controlled room (22 ± 1 °C) with free access to water and a standard rodent chow (CRF-1, Charles River Laboratories, Japan) or CRF-1 containing 0.5 mg/kg day^{-1} of topiroxostat (Sanwa Kagaku Kenkyusho, Japan) for 2 weeks prior to experiments.

2.2. Measurement of hemodynamics

Rats were anesthetized with isoflurane (2.5%) with supplemental oxygen (1 L / minute), intubated and ventilated by a rodent respirator (model 683, Harvard Apparatus, South Natick, MA). Cardiac function was analyzed using a catheter-tip manometer (Miller Instruments, Houston, TX) and a conductance catheter (Unique Medical, Tokyo, Japan) inserted into the LV cavity through the right carotid artery. Integral 3 (Unique Medical) was used to store data from the tip-manometer and to calculate systolic and diastolic functional parameters. The left ventricular (LV) pressure-volume relationship (PVR) was determined as previously reported [5]. Hemodynamic data were obtained at baseline and 3 min after LV end-systolic pressure (LVESP) had been elevated to 200 mmHg by gradual titration of continuous infusion of phenylephrine. These hemodynamic analyses were performed blindly in OLETF and LETO that were randomly assigned to a pretreatment with ($n = 9$ and $n = 8$, respectively) or without (n = 9 and $n = 7$, respectively) per oral administration of topiroxostat.

2.3. Measurement of AMP deaminase (AMPD) activity

AMPD activity in the heart tissue was measured as previously described [5,6].

2.4. Measurements of purine metabolites, XOR activity and activity of hypoxanthine phosphoribosyl transferase (HPRT)

ATP content in the myocardium was measured using an ATP colorimetric/fluorometric assay kit (BioVision Inc., Milpitas, CA). Left ventricular tissues were homogenized in phosphate buffered saline (pH 7.4) containing protease inhibitor cocktail (Roche, Basel, Switzerland) and centrifuged at 20,000*g* for 20 min at 4 °C. For the determination of purine bases, these homogenates or plasma were added to methanol containing [$^{13}C_2$,$^{15}N_2$]-xanthine, [$^{13}C_3$,^{15}N]-hypoxanthine and [$^{13}C_2$,$^{15}N_2$]-UA as internal standards. The resulting suspensions were centrifuged at 3000 *g* for 15 min at 4 °C. The supernatants were 5-fold diluted with distilled water and filtered through an ultrafiltration membrane (AcroPrep Advance Filter Plate for Ultrafiltration, Omega 3 K MWCO, PALL), and purine bases were measured using liquid chromatography/triple quadrupole mass spectrometry (LC/TQMS, Nexera/QTRAP4500, SHIMADZU/SCIEX). Activity of XOR was measured by the method described previously [26,27] with slight modification. In brief, the heart homogenates, kidney homogenates or plasma were added to a mixture containing [$^{13}C_2$,$^{15}N_2$]-xanthine (0.667 μmol/l), NAD^+ (0.133 μmol/l), and oxonate (0.013 mmol/l) in 20 mmol/l Tris buffer (pH 8.5) and were incubated at 37 °C for 30 min. Methanol containing [$^{13}C_2$, $^{15}N_2$]-UA was added to the mixture, and then the mixture was centrifuged at 3000 *g* for 15 min at 4 °C. The supernatants were dried using a centrifugal evaporator, and the precipitates were reconstituted with 150 μlL distilled water. The amounts of [$^{13}C_2$,$^{15}N_2$]-UA production were measured using LC/TQMS (Nexera/QTRAP4500, SHIMADZU/SCIEX), and activity of XOR was expressed as [$^{13}C_2$, $^{15}N_2$]-UA nmol/min/mg protein.

Enzyme activity of HPRT in the myocardium was measured using PicoProbe™ Hypoxanthine Phosphoribosyl Transferase Activity Assay Kit (BioVision).

2.5. Measurement of oxidative stress

As indices of oxidative stress, areas stained with anti-4-hydroxynonenal (4-HNE) antibody in ventricular sections, tissue levels of malondialdehyde (MDA) and 4-HNE, and tissue level of proteins carbonylation were determined by using methods described in Supplementary Methods. Tissue level of advanced glycation end-products (AGE) that reportedly regulates ROS was also determined by using OxiSelect Advanced Glycation End Product Competitive ELISA Kit (Cell

Biolabs, Inc., San Diego, CA). ROS levels in H9c2 cells were monitored by 2′-7′-dichlorofluorescein (DCF) fluorescence.

2.6. Nonheme iron assay

Nonheme iron contents in the cytosolic and mitochondrial fractions in the heart were measured as previously described [24].

2.7. Immunoblotting

Proteins in the myocardial samples were determined by immunoblotting using snap-frozen heart tissues as previously reported [5,6]. Antibodies used in this study were as follows: XDH (55156-1-AP, Proteintech, IL); AMPD3 (23997-1-AP, Proteintech, IL); NOX2 (ab129068, Abcam, UK); NOX4 (ab133303, Abcam); catalase (C0979, Sigma-Aldrich, St Louis, MO); MnSOD (06–984, Merck Millipore, Burlington, MA); VDAC1 (ab14734, Abcam); and vinculin (V9131, Sigma-Aldrich).

2.8. Immunoprecipitation of AMPD3

Precleared cell lysates (500 μg) were incubated with 2 μg of anti-AMPD3 antibody (sc398548, Santa Cruz Biotechnology, Dallas, TX) in IP buffer (20 mM Tris–HCl [pH 7.4], 1 mM EGTA, 5 mM NaN_3, 50 mM NaCl, 1 mM PMSF, 50 mM Na_3VO_4, 1% Triton X-100, 0.5%NP-40 and a protease inhibitor cocktail) at 4 °C overnight with rotation. The antibody-AMPD3 complex was collected with magnet beads and washed with IP buffer. The immunoprecipitates were subjected to immunoblotting using anti-phospho-Thr antibody (#9318, Cell Signaling Technology, Danvers, MA).

2.9. Cell culture and transfection

H9c2 cells (American Type Culture Collection) were cultured in DMEM supplemented with 10% FBS at 37 °C with 5% CO_2. The cells were used for experiments when they were 70–90% confluent. miRNA inhibitors for miR-301b were purchased from Exiqon (Valencia, CA) and transfected at a final concentration of 25 nmol/l in the H9c2 cells using Lipofectamine® RNAiMAX Reagent (Invitrogen, Carlsbad, CA) according to the manufacturer's recommendations. To generate an expression vector for FLAG-tagged AMPD3, the coding region of AMPD3 was amplified from rat cDNA by PCR using KOD-Plus- Ver. 2 (Toyobo, Osaka, Japan) and the following primers: 5′-AAAAGCGGCCGCGATGCGCGCGCCCGTGTGTG-3′ (forward) and 5′-AAAAGGATCCCCTAGTCCGCCAGGGCTGTGATC-3′ (reverse). The PCR fragment was cloned into NotI and BamHI sites of p3xFLAG-CMV™-7.1 expression vector (Sigma-Aldrich). The cDNA sequence was verified by nucleotide sequencing. FLAG-AMPD3 or FLAG-control vector was transfected in the H9c2 cells using FuGENE HD (Promega, Madison, WI) according to the manufacturer's recommendations.

2.10. Measurement of mitochondrial respiration

Mitochondrial oxygen consumption rate was measured in isolated mitochondria from rat hearts by Seahorse XFe96 Analyzer (Agilent Technologies) as previously described with slight modifications [24].

2.11. Statistics

Group mean data are shown as means ± S.E. One-way analysis of variance was used to test differences among group mean data. When analysis of variance indicated a significant overall difference, multiple comparisons were performed using the Tukey-Kramer post-hoc test. The difference was considered to be statistically significant if p was less than 0.05.

3. Results

3.1. Distinct responses of hemodynamic parameters to pressure overload in OLETF and LETO and their modification by inhibition of XOR

We first confirmed a diabetic phenotype of OLETF and cardiac dysfunction at the age of 29–35 weeks. As in our previous studies [5,6,21], OLETF showed significantly larger body weight and higher plasma glucose level than those of LETO as shown in Supplementary Table 1. In our previous studies, we repetitively confirmed elevation of plasma glucose, serum triglycerides and plasma insulin levels in OLETF at the age of 29–35 weeks compared with those in LETO [5,6,19,25], and insulin resistance in OLETF at the same ages was demonstrated by the glucose clamp method [25]. Thus, we did not determine all of the plasma metabolic parameters in the present study. Under a conscious condition, heart rates were comparable in OLETF and LETO, but blood pressure was significantly higher in OLETF than in LETO (Supplementary Table 1). To examine the involvement of XOR in diastolic dysfunction in OLETF, we first determined XOR activity in the tissue and the effect of topiroxostat, a selective inhibitor of XOR [26], on LV function in OLETF and LETO. The activity of XOR in the LV myocardium, plasma and kidney was significantly higher in OLETF than in LETO in an unstimulated condition (Supplementary Fig. S1). Administration of topiroxostat dose-dependently inhibited XOR activity in the LV myocardium, plasma and kidney (Supplementary Fig. S1). Since administration of topiroxostat at the highest dose tested, 0.5 mg/kg/day, for 14 days had no effect on body weight, plasma glucose level, heart rate or blood pressure (Supplementary Table 1), we chose the dose of 0.5 mg/kg/day for subsequent experiments.

In pressure-volume loop analysis, tau and LVEDP were comparable in OLETF and LETO at baseline (Fig. 1A and B). Similarly, there was no significant difference in end-systolic elastance (Ees), dP/dtmax, arterial elastance (Ea) or Ea/Ees, an index for ventricular-arterial coupling, in OLETF and LETO at baseline (Fig. 1C-F). We next attempted to confirm different responses of the hemodynamic parameters to pressure overload in OLETF and LETO, which we previously reported [5,6], and to examine whether the responses are modified by treatment with topiroxostat. Four rats (2 LETO, 1 LETO treated with topiroxostat and 1 OLETF) were excluded from the experiment as systolic blood pressure was below 90 mmHg during stabilization before pressure-volume relationship measurement, and the remaining 33 rats were included in the analyses. OLETF and LETO underwent continuous intravenous infusion of phenylephrine for elevation of blood pressure to 200 mmHg. During the pressure overload, tau was significantly prolonged (from 8.0 ± 0.4 to 14.7 ± 0.8 and from 6.1 ± 0.2 to 12.5 ± 0.7 msec) and LVEDP was significantly elevated (from 5.6 ± 0.4 to 18.3 ± 1.5 and from 4.7 ± 0.7 to 12.1 ± 1.3 mmHg) in both OLETF and LETO. Under the condition of pressure overload, LVEDP in OLETF was significantly higher than that in LETO (Fig. 1B) and tau also tended to be higher in OLETF than in LETO (Fig. 1A). Treatment with topiroxostat significantly improved both tau (from 14.7 ± 0.8 to 11.8 ± 0.8 msec, Fig. 1A) and LVEDP (from 18.3 ± 1.5 to 11.3 ± 1.1 mmHg, Fig. 1B) in OLETF but not in LETO, while it did not significantly change the parameters before pressure overloading. Ees and dP/dtmax were also significantly increased by the pressure overload to comparable levels in OLETF and LETO (Fig. 1C and D). Topiroxostat tended to increase Ees in OLETF, though the effect did not reach statistical significance (Fig. 1C). Pressure overload-induced increase in Ea was not significantly affected by topiroxostat in OLETF and LETO (Fig. 1E). A significant increase in Ea/Ees under the condition of pressure overload was also observed in both OLETF and LETO (Fig. 1F), with OLETF showing significantly higher Ea/Ees than that in LETO. Administration of topiroxostat abolished the pressure overload-induced increase in Ea/Ees in OLETF, but not in LETO (Fig. 1F). These findings indicate that XOR plays a role in the pressure overload-induced deterioration of diastolic function and ventricular-arterial coupling in diabetic hearts.

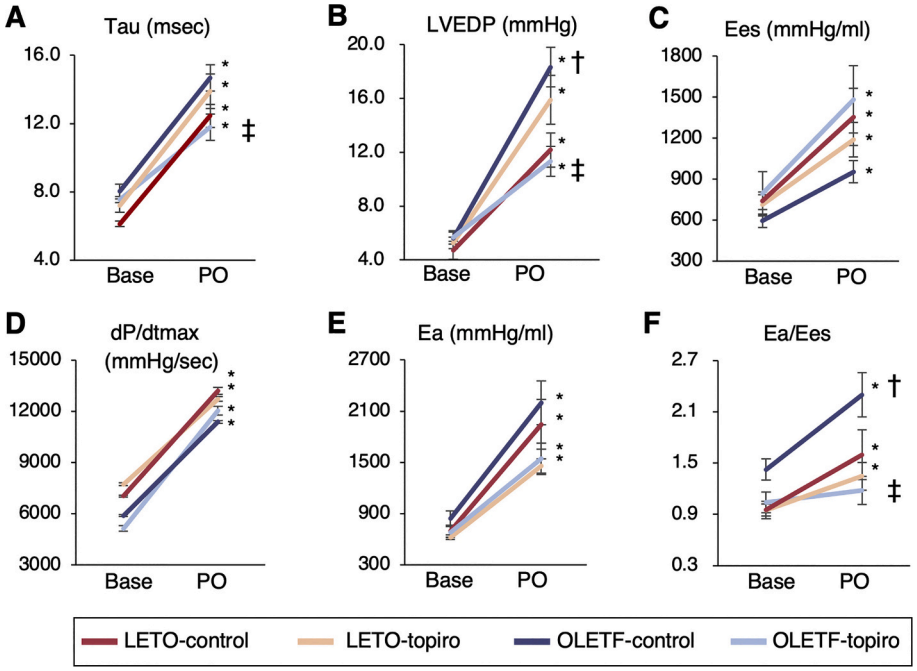

Fig. 1. Hemodynamic response to pressure overload with or without treatment with topiroxostat (0.5 mg/kg/day). Summary of changes in tau (A), left ventricular end-diastolic pressure (LVEDP) (B), end-systolic elastance (Ees) (C), dP/dtmax (D), effective arterial elastance (Ea) (E), and ventricular-arterial coupling (Ea/Ees) (F) in LETO and OLETF. Rats were exposed to pressure overloading of 200 mmHg (PO) by phenylephrine infusion. N = 7–9 in each group. *p < 0.05 vs. baseline, † p < 0.05 vs. LETO-control, ‡ p < 0.05 vs. OLETF-control. Base, baseline. PO, pressure overload. Topiro, topiroxostat.

3.2. *Distinct involvement of pressure overload and XOR on modification of purine metabolic pathways in OLETF and LETO*

To test our hypothesis that upregulated AMPD augments the pathological role of XOR, we examined the relationships between AMPD, XOR and the purine metabolic pathway in the pressure overload-induced cardiac dysfunction in T2DM hearts. Consistent with the results of our previous studies [5,6], activity of AMPD was significantly higher in OLETF than in LETO both at baseline and under the condition of pressure overload (Fig. 2A). At baseline, XOR activity level was higher in OLETF than in LETO (Fig. 2B), while there was no significant difference between hypoxanthine, xanthine and uric acid levels in the two groups (Fig. 2C-E). Interestingly, pressure overload significantly increased XOR activity and levels of xanthine and uric acid in both LETO

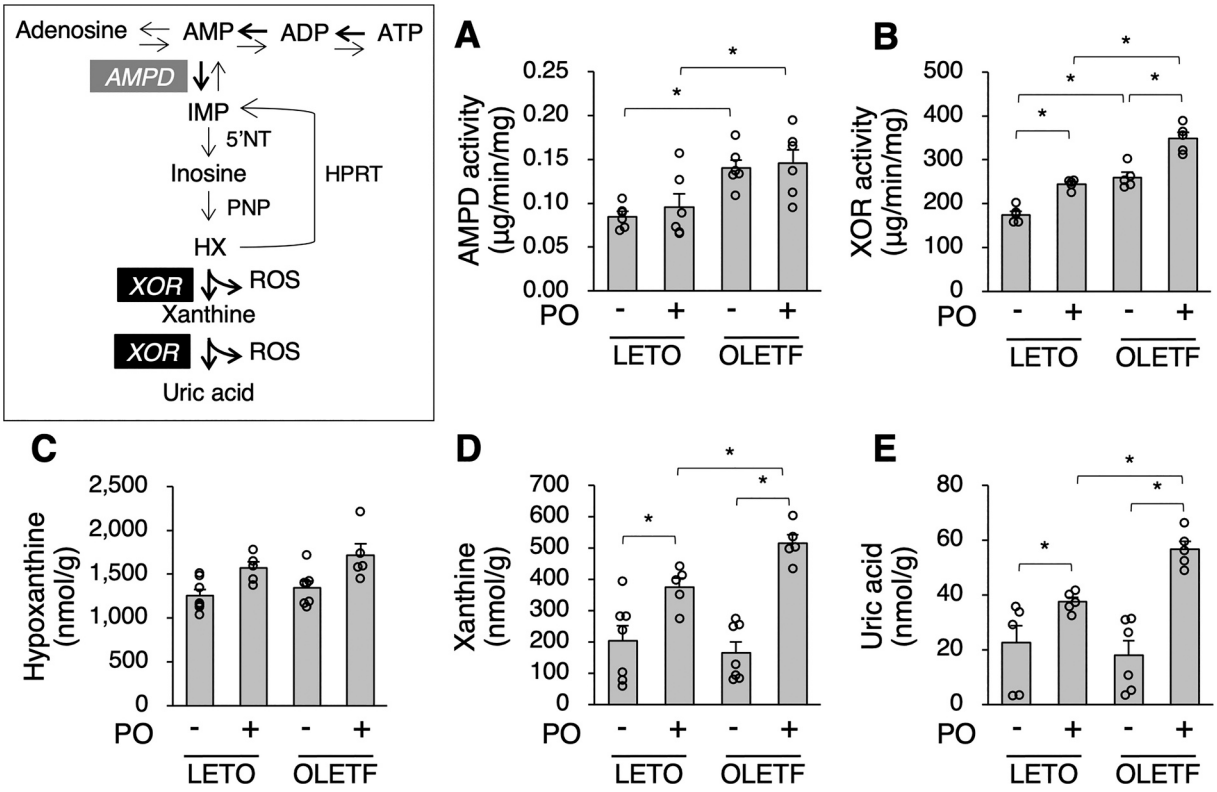

Fig. 2. Effects of phenylephrine-induced pressure overload on purine metabolic pathways. Activity of AMPD (A), activity of XOR (B), and levels of hypoxanthine (C), xanthine (D) and uric acid (E) in the presence or absence of pressure overload are shown. PO, pressure overload. N = *4–6 in each group.* *p < 0.05.

and OLETF, and the magnitude of changes was larger in OLETF than in LETO (Fig. 2B, D-E). The levels of hypoxanthine were comparable in OLETF and LETO at baseline and the difference in hypoxanthine level between the two groups did not reach statistical significance under the condition of pressure overload (Fig. 2C). The results appear to contradict upregulation of AMPD in OLETF but are possibly explained by an adaptive response of the hypoxanthine-guanine phosphoribosyl transferase (HPRT)-mediated purine salvage pathway [27] (detailed discussion in Section 4.4).

Treatment with topiroxostat did not alter the activity of AMPD (Fig. 3A), while it significantly inhibited myocardial XOR activity both in OLETF and LETO (Fig. 3B). During the pressure overloading, ATP level in the LV myocardium was significantly lower and levels of xanthine and uric acid were higher in OLETF than in LETO (Fig. 3C, E and F), while hypoxanthine levels were similar in the two groups (Fig. 3D). These changes in tissue metabolite levels by pressure overloading in OLETF were attenuated by topiroxostat.

3.3. Inhibition of XOR abolishes the increase in the level of oxidative stress in OLETF

A significantly higher level of oxidative stress in the myocardium under the condition of pressure overload in OLETF than in LETO was indicated by higher tissue levels of 4-HNE immunoreactivity (Fig. 4A) and MDA plus 4-HNE (Fig. 4B), indices for lipid peroxidation, and levels of carbonylated proteins (Fig. 4C). We also determined the level of AGE, since it has been reported to be upregulated by diabetic conditions and to regulate ROS in a bidirectional fashion [28,29]. As shown in Supplementary Fig. S2, the level of AGE in the myocardium tended to be higher in OLETF than in LETO, but the difference was not statistically significant. Levels of AGE in both OLETF and LETO were not changed by topiroxostat. In contrast, the elevations in 4-HNE immunoreactivity and MDA + 4-HNE levels and increased protein carbonylation in OLETF were attenuated by topiroxostat (Fig. 4A-C), indicating a major role of XOR in increased oxidant stress.

In contrast to XOR activity, protein levels of nicotinamide adenine dinucleotide phosphate oxidase (NOX)2, NOX4, manganese superoxide dismutase (MnSOD) and catalase in the myocardium were not significantly different in OLETF and LETO (Supplementary Fig. S3), arguing against their roles in increased oxidative stress in the myocardium of OLETF.

3.4. Increased AMPD contributes to the upregulation of XOR activity in OLETF under the condition of pressure overload

To explore the mechanisms underlying the upregulated XOR activity in OLETF (Fig. 2B), we examined the protein level of XOR and its relationship with AMPD3. As shown in Fig. 5A, OLETF showed 16% higher XOR protein level than did LETO under the condition of pressure overload, regardless of treatment with topiroxostat. We examined whether increased expression of AMPD3 is causally related to elevation of XOR protein level in OLETF. H9c2 cells were transfected with Flag-tagged AMPD3 and the expression level of XOR was analyzed. Despite the markedly elevated level of AMPD3 protein after transfection of Flag-AMPD3 (Fig. 5B), XOR protein level was unaffected (Fig. 5C). Next, we examined the possibility that AMPD3 and XOR were simultaneously regulated by miR-301b. This possibility was postulated since we previously found that down-regulation of miR-301b is responsible for AMPD3 upregulation in diabetic hearts [6], and TargetScan, an algorithm for finding genomic targets for the miRNAs, predicted binding of miR-301b to the 3'UTR of XOR mRNA. However, transfection of an miR-301b inhibitor at a dose that increased AMPD by 4.7 fold did not change XOR protein level in H9c2 cells (Fig. 5D and E). Because a relatively small increase in XOR protein levels was unlikely to entirely explain the elevation of XOR activity, we next postulated that increase in the amount of inosine upregulates XOR activity in the myocardium, as

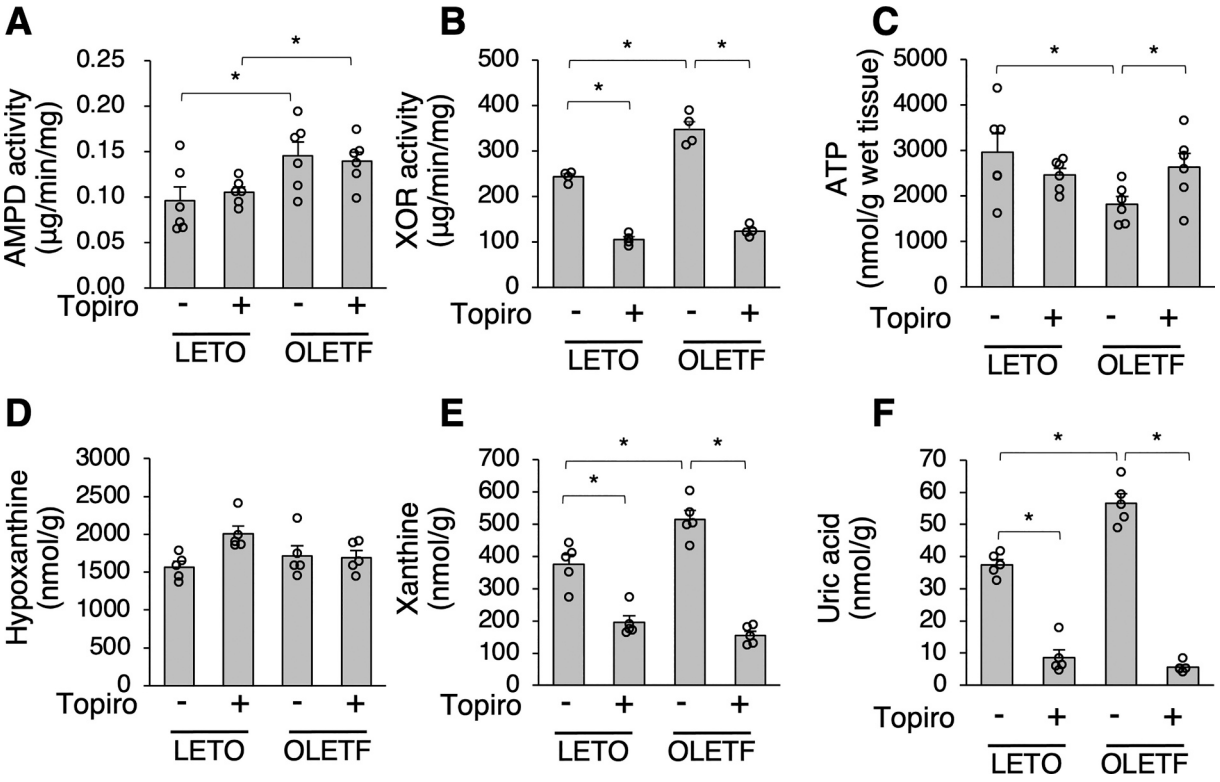

Fig. 3. Effects of topiroxostat on purine metabolic pathways under the condition of pressure overload. Activity of AMPD (A), activity of XOR (B), and levels of ATP (C), hypoxanthine (D), xanthine (E) and uric acid (F) in the presence or absence of topiroxostat are shown. N = 4–6 in each group. *p < *0.05*.

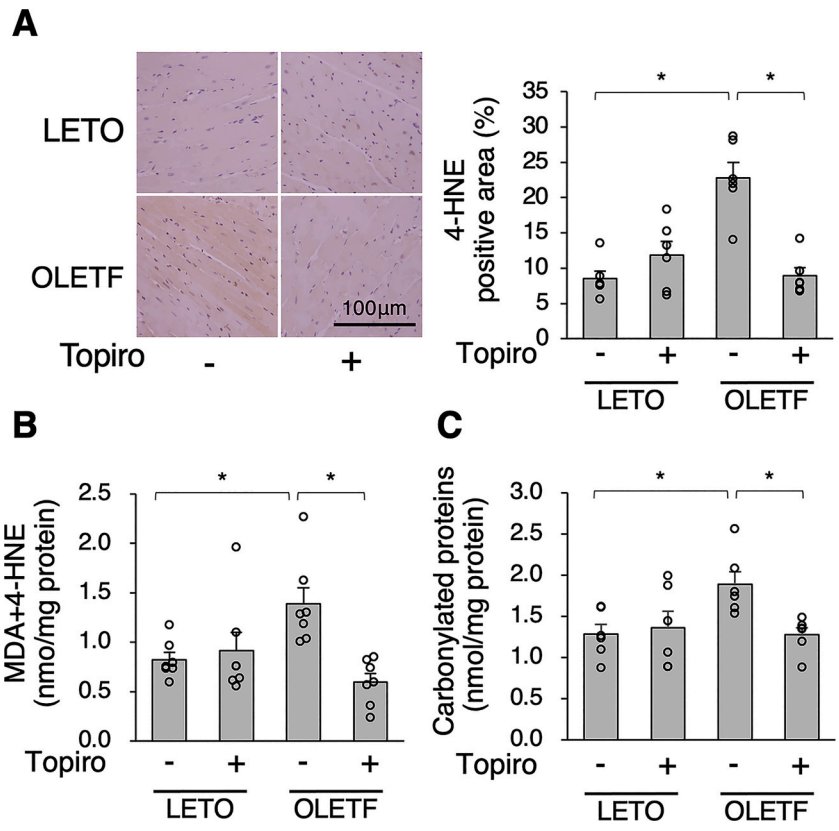

Fig. 4. Effects of topiroxostat on oxidative stress in the left ventricular myocardium. (A) Representative images of left ventricular sections stained with anti-4-hydroxynonenal (4-HNE) antibody under the condition of pressure overload with or without treatment with topiroxostat (top panels) and quantitative analysis of 4-HNE-positive areas (bottom panels). (B) Level of malondialdehyde (MDA) plus 4-HNE and (C) protein carbonylation in the LV myocardium under the condition of pressure overload with or without treatment with topiroxostat. N = 5–7 in each group. * $p < 0.05$.

demonstrated in chick liver tissue [30]. Indeed, our previous metabolomic analyses demonstrated that tissue inosine level during pressure overloading was 1.2-fold higher in OLETF than in LETO, while the difference was statistically insignificant at the baseline condition [5]. Thus, we measured the activity of XOR in LV homogenates obtained from LETO and OLETF with or without addition of exogenous inosine. As shown in Fig. 5F, the activity of XOR was significantly augmented by addition of inosine at the final concentration of 300 μmol/L, which is estimated to mimic the increase in endogenous inosine in OLETF under the condition of pressure overload [5]. Thus, it is plausible that increased AMPD in OLETF contributes to upregulation of XOR activity under the condition of pressure overload via an increased level of inosine.

Since phosphorylation of XOR on Thr222 by CDK5 has been reported to contribute to hypoxia-induced hyperactivation of XOR in the lung [31], we determined the levels of phospho-Thr of XOR in LETO and OLETF. Anti-XOR immunoprecipitates obtained from the myocardia of LETO and OLETF were separated by SDS-PAGE followed by immunoblotting with anti-phospho-Thr antibody. As shown in Supplementary Fig. S4, no difference was observed between LETO and OLETF in the level of phospho-Thr of XOR in XOR-immunoprecipitates, arguing against the possibility that increased activity of XOR in the heart of OLETF was mediated by Thr-phosphorylation.

Cellular iron level has also been shown to be critical for regulation of XOR activity [32,33]. However, the levels of iron in either the cytosol or mitochondrial fraction of the LV myocardium were similar in OLETF and LETO, regardless of treatment with topiroxostat (Supplementary Fig. S5).

We next examined whether overexpression of AMPD3 indeed promotes purine generation, augments ROS production and reduces ATP level. The level of hypoxanthine was modestly but significantly higher in H9c2 cells transfected with FlAG-AMPD3 than in H9c2 cells transfected with a FLAG-control vector (Fig. 6A), though the levels of xanthine and uric acid were below the measurement sensitivity. The level of ROS analyzed by DCF staining was significantly higher (Fig. 6B) and the level of ATP was significantly lower (Fig. 6C) in FLAG-AMPD3-transfected cells than in control vector-transfected cells. These findings indicate that there is a causal relationship between increased activity of AMPD, promoted purine generation, and excess ROS production.

3.5. *Impaired mitochondrial state 3 respiration in OLETF is restored by XOR inhibition*

To investigate the mechanisms by which increased XOR activity in diabetic hearts is associated with depletion of myocardial ATP during pressure overload (Fig. 3B and C), we analyzed the respiratory chain function in mitochondria freshly isolated from OLETF and LETO using the Seahorse X96 analyzer. Mitochondria isolated from the LV myocardium of OLETF showed a significant decrease in ADP-stimulated state 3 respiration compared to that in LETO (Fig. 7A and B), whereas ADP-limited state 4 respiration levels were similar in the two groups (Fig. 7A and B). The maximal rate of oxidative phosphorylation measured after addition of the mitochondrial uncoupler FCCP (state 3-u) was also significantly lower in OLETF than in LETO (Fig. 7A and B). Treatment with topiroxostat significantly improved the state 3 and state 3-u respiration in OLETF mitochondria. These results are consistent with restoration of myocardial ATP level in OLETF by topiroxostat (Fig. 3C).

3.6. *Effects of pressure overloading and topiroxostat on HPRT activity in the myocardium*

Since HPRT plays roles in purine salvage and preservation of ATP level, we examined differences in HPRT activity in the myocardium between LETO and OLETF. There was no significant difference in the activity of HPRT in the myocardium between OLETF and LETO regardless of pressure overloading or treatment with topiroxostat

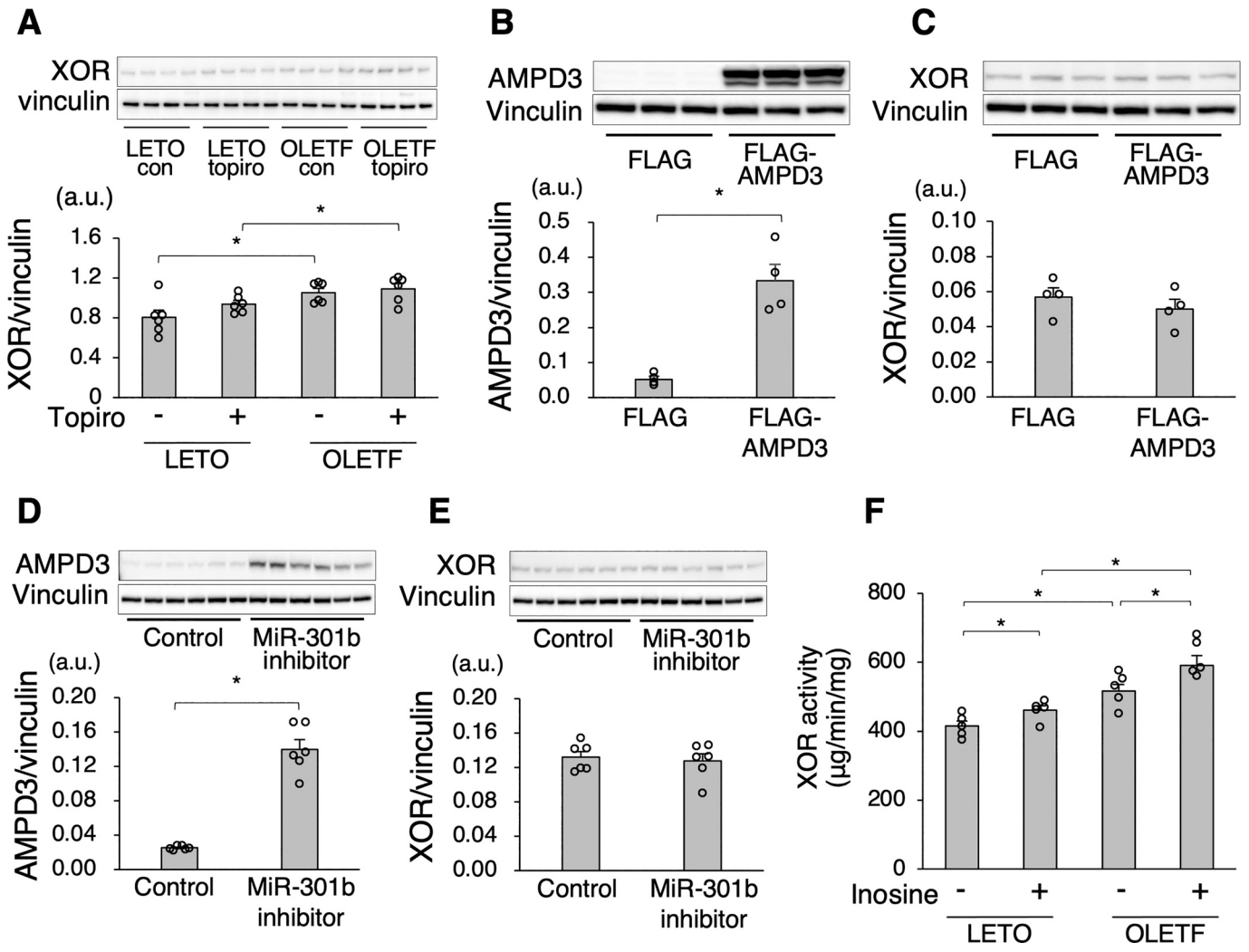

Fig. 5. Lack of change in XOR protein level by a XOR inhibitor or by AMPD3 protein level and effects of exogenous inosine on activity of XOR in LV myocardial homogenates. (A) Representative immunoblot (top) and summary data (bottom) for vinculin-normalized protein levels of XOR with or without treatment with topiroxostat. Representative immunoblot (top) and summary data (bottom) for vinculin-normalized protein levels of AMPD3 and XOR in H9c2 cells transfected with FLAG-tagged AMPD3 (B and C) or miR-301b inhibitor (D and E). (F) Activity of XOR in OLETF and LETO and augmentation of their activity by addition of inosine at a final concentration of 300 μmol/L. N = 4–6 in each group. Topiro, topiroxostat. * $p < 0.05$.

(Supplementary Fig. S6).

4. Discussion

4.1. Functional link between AMPD and XOR in ROS-mediated injury in diabetic hearts

The results of the present study indicate for the first time a close functional link between AMPD and XOR in the pathogenesis of diabetic cardiomyopathy. Although XOR protein expression is regulated independently from the AMPD protein level, XOR activity was stimulated by inosine, a product of AMPD-mediated metabolic pathway. The contribution of XOR-derived ROS to mitochondrial dysfunction in the diabetic heart was shown by the findings that treatment with a XOR inhibitor, topiroxostat, significantly decreased tissue levels of 4-HNE, MDA and carbonylated proteins and suppressed mitochondrial dysfunction. Importantly, the level of myocardial XOR activity was further elevated during LV pressure overloading as expected from the increase in formation of substrates via the AMPD-mediated pathway. Furthermore, the impact of pressure loading on XOR activity was much larger in the diabetic heart. Inhibition of XOR by topiroxostat ameliorated the adverse effects of pressure overloading on purine metabolites, mitochondrial function, tissue ATP level and LV diastolic function in the diabetic heart. These protective effects of topiroxostat were observed in the myocardium of OLETF, in which AMPD expression is upregulated, but not in the myocardium of LETO, a non-diabetic control. Taken together, the present findings indicate that upregulated AMPD activity contributes to aggravation of LV contractile dysfunction at the time of increased LV workload not only by increased deamination of AMP but also by enhanced ROS-mediated mitochondrial injury via increases in both XOR activity and formation of its substrates (Fig. 8).

4.2. Mechanisms underlying diabetes-induced respiratory chain dysfunction

An association of LV contractile dysfunction in diabetic hearts with impaired mitochondrial function has been demonstrated by the use of different animal models of diabetes mellitus [1], and the mechanisms of mitochondrial dysfunction differ depending on the etiology of diabetes mellitus and stage of diabetic cardiomyopathy. For example, in the hearts of ob/ob mice, suppression of mitochondrial state 3 respirations due to reduction in the protein levels of electron transport chain

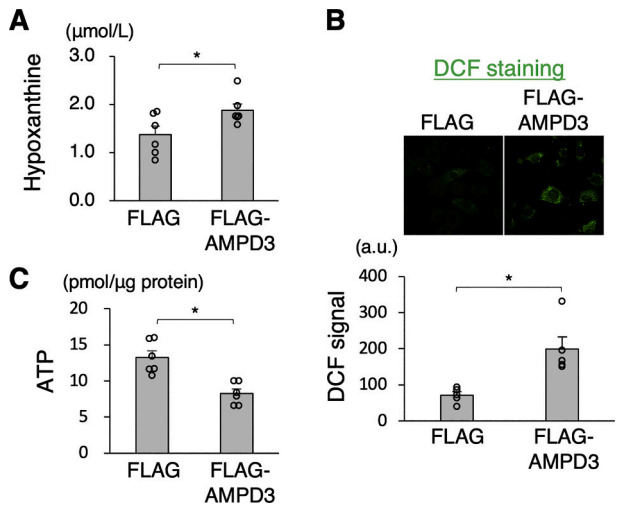

Fig. 6. Effects of AMPD3 overexpression on the levels of hypoxanthine, oxidant stress and ATP in H9c2 cells. The levels of hypoxanthine (A), oxidant stress determined by DCF staining (B) and ATP (C) in H9c2 cells transfected with FLAG-tagged AMPD3 or FLAG-control vector.

complex and mitochondrial uncoupling have been reported [34]. On the other hand, db/db mice showed excess ROS production promoted by downregulation of the F1α-subunit of ATP synthase and fatty acid-induced mitochondrial uncoupling [35] and a decrease in state 3 and state 4 respiration [36]. In the present study, we postulated that ROS production augmented by upregulated XOR-catalyzed reaction induces mitochondrial respiratory chain dysfunction in diabetic cardiomyopathy at a stage when systolic function is preserved [5]. The postulation is based on reports that activities of mitochondrial respiratory complexes I, II, and IV were diminished by oxidant stress [37,38]. In fact, inhibition of XOR by topiroxostat significantly attenuated oxidative stress (Fig. 4), preserved myocardial ATP level (Fig. 3C) and improved ventricular function during pressure loading (Fig. 1) in OLETF. State 3, but not state 4, respiration in vitro was impaired in mitochondria isolated from OLETF compared to those in mitochondria from LETO (Fig. 7). Oxygen consumption at the time of FCCP treatment was also reduced in OLETF mitochondria, indicating that the impaired state 3 respiration in OLETF was attributable to a defect in electron transfer from complex I to complex IV but not in F1/F0 ATP synthase.

4.3. Mechanisms by which XOR activity and protein are upregulated in diabetic hearts

Upregulated activity of AMPD indirectly contributes to augmented activity of XOR through elevation of inosine level (Fig. 5F and Fig. 8). On the other hand, upregulated AMPD activity could also be associated with increased expression of XOR protein in OLETF. However, overexpression of AMPD3 in H9c2 cells did not alter the expression levels of XOR, excluding the possibility of XOR protein expression being regulated by AMPD activity (Fig. 5B and C). Besides, the possibility that miR-301b suppresses expression of both AMPD3 and XOR as a common translational regulator was also excluded, as transfection of H9c2 cells with miR-301b inhibitor did not alter the level of XOR protein (Fig. 5D and E). Among 57 miRNAs that were shown to be downregulated (≥50%) in OLETF compared to LETO by miRNA array analysis [6], there was no other mi-RNA that is predicted to bind to 3'UTR of both XOR mRNA and AMPD mRNA. Thus, it is unlikely that XOR and AMPD share common miRNAs that simultaneously contribute to the translational regulation of both proteins in diabetic hearts. On the other hand, it is possible that some transcriptional regulation plays a role in upregulation of both XOR and AMPD3. For example, it has been reported that mRNA and protein levels of TNF-α were significantly greater in db/db mouse hearts compared to those in the wild type mice [39]. Although not in cardiomyocytes, Pfeffer et al. demonstrated that transcription of XOR was upregulated in bovine renal epithelial cells when treated with TNFα [40]. On the other hand, upregulation of AMPD3 transcript after ischemia/reperfusion in the lung was associated with the increased protein level of TNFα [41]. These findings suggest that TNFα is upregulated in diabetic hearts, possibly contributing to simultaneously increased protein level of XOR and AMPD3.

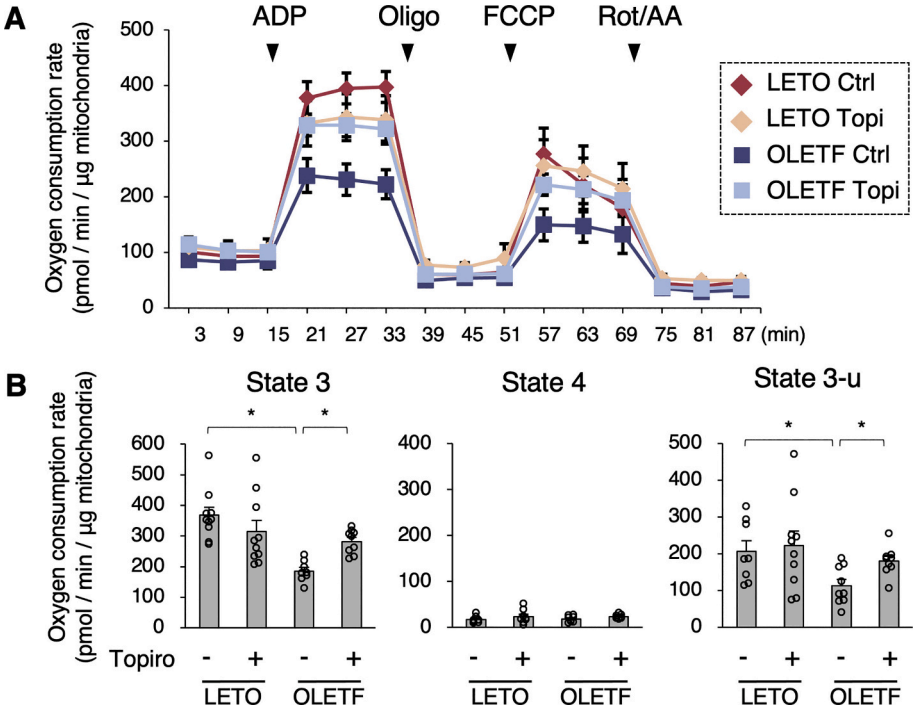

Fig. 7. Effects of topiroxostat on respiratory chain function in LV myocardial mitochondria. (A) Oxygen consumption rate determined by the Seahorse XFe96 analyzer in mitochondria isolated from OLETF or LETO in the presence or absence of treatment with topiroxostat. (B) State 3 respiration indicates oxygen consumption with ADP, state 4 indicates respiration with oligomycin, and state 3u indicates uncoupled respiration with carbonylcyanide-4-trifluoromethoxyphenylhydrazone (FCCP). N = 8–10 in each group. Topiro, topiroxostat. * $p < 0.05$.

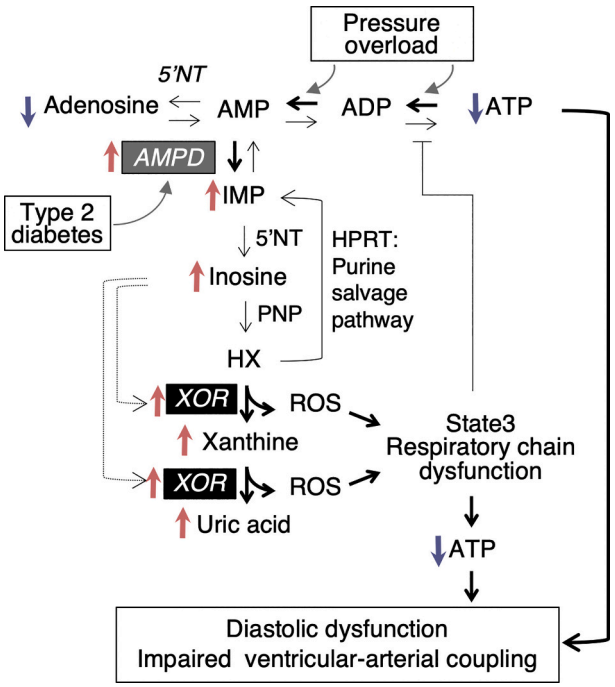

Fig. 8. Schematic diagram of the pathophysiological consequences of pressure overload in type 2 diabetic hearts. Pressure overload promotes consumption of ATP, leading to accumulation of AMP. Upregulated AMPD in diabetic hearts deaminates AMP, resulting in increased production of IMP. In a physiological context, removal of accumulated AMP under the condition of high ATP turnover prevents reduction of phosphorylation potential. Simultaneously, excess degradation of AMP by AMPD leads to depletion of the adenine nucleotide pool and reduction of ATP level. IMP is converted to inosine by 5′-nucleotidase (5'NT), and inosine is in turn converted to hypoxanthine (HX) by purine nucleoside phosphorylase (PNP), providing XOR with its substrates. In diabetic hearts with upregulated AMPD, increase in ventricular workload by pressure overloading induces elevation of the AMP level as well as elevation of the levels of IMP and inosine, the latter of which contributes to the increase in activity of XOR. Increases in the formation of substrates and enzymatic activity of XOR contribute to production of excessive ROS, leading to mitochondrial respiratory chain dysfunction and decrease in ATP production in diabetic hearts. State 3 respiratory chain dysfunction and impaired ATP synthesis may also partially contribute to AMP accumulation, possibly forming a vicious circle.

4.4. *Effects of AMPD upregulation on tissue HX and xanthine levels*

The findings that myocardial levels of hypoxanthine and xanthine were not significantly different between OLETF and LETO without pressure overloading (Fig. 2) may appear to contradict our hypothesis that upregulated AMPD amplifies the role of XOR. However, the findings can be explained by the capacity of HPRT, which catalyzes production of IMP from hypoxanthine. Levels of inosine and other purines levels, AMP, IMP or total adenine nucleotide pools in the myocardium were similar in OLETF and LETO without LV pressure overloading, and baseline ventricular function was comparable in the two groups in our previous [5] and the present (Fig. 1 and Fig. 3) studies, suggesting that phosphorylation of adenine nucleotides and preservation of nucleotides were achieved by mitochondrial ATP generation and HPRT-mediated purine salvage pathways. In contrast, under the condition of pressure overloading that increased rate-pressure products, an index of myocardial oxygen consumption, by approximately two fold, there was a significantly larger increase in XOR activity in OLETF than in LETO (Fig. 2), while HPRT activity was unchanged in both groups (Supplementary Fig. S6). LV pressure overloading was shown to increase tissue IMP and inosine and to reduce the adenine nucleotide pool in the myocardium of OLETF in our previous study [5]. Furthermore, topiroxostat treatment significantly reduced the xanthine level without increasing the hypoxanthine level in the myocardium under the condition of pressure overload (Fig. 3D and E). Taken together, alterations in hypoxanthine and xanthine levels during pressure overloading in OLETF can be explained by the combined effects of upregulated AMPD activity, increased AMP turnover rate, and inosine-mediated upregulation of XOR activity that competed with HPRT for hypoxanthine.

4.5. *Possible involvement of HPRT-1 in topiroxostat-mediated amelioration of pressure overload-induced diastolic dysfunction in OLETF*

A recent study by Fujii et al. [42] suggested that acceleration of the purine salvage pathway, which utilizes hypoxanthine to restore the adenine nucleotide pool, contributes to the protective effect of a XOR inhibitor, febuxostat, on ischemia/reperfusion injury in the kidney. In their study, febuxostat pretreatment promoted recovery of ATP level after reperfusion and attenuated ischemia/reperfusion-induced injury in the murine kidney. Interestingly, the renoprotective effect afforded by febuxostat was canceled by silencing the HPRT-1 gene in cultured renal tubular cells [42]. In the present model of pressure overload-induced ventricular dysfunction, activity of HPRT was not correlated with the severity of diastolic dysfunction or with the protective effect of topiroxostat in OLETF (Supplementary Fig. S6). Thus, HPRT activity is unlikely to be primarily responsible for protective effects of topiroxostat on ventricular dysfunction, though its permissive role cannot be excluded.

4.6. *Results of the EXACT-HF does not necessarily argue against the effect of XOR inhibition in diabetic hearts*

The effect of a XOR inhibitor on the clinical outcome in a high-risk heart failure population with elevated serum uric acid was examined in the EXACT-HF trial [43]. As opposed to the hypothesis based on results of observational clinical studies [13,14,44], treatment with allopurinol failed to suppress primary composite clinical endpoint (i.e., survival, worsening heart failure, and patient global assessment). However, the negative results of the EXACT-HF trial do not necessarily argue against the presence of XOR-mediated myocardial injury in a subgroup of patients with heart failure. Hyperuricemia, one of the inclusion criteria for the EXACT-HF trial (serum uric acid $\geq$9.5 mg/dL), occurs as a result of increased uric acid production, impaired renal uric acid excretion, or their combination [45]. In addition, uric acid is a major ROS scavenger in the extracellular space [46]. Thus, uric acid level is unlikely to be a good biomarker to identify patients at high risk for XOR-derived ROS-mediated cardiovascular injury. The present study showed that XOR activity is upregulated by diabetes as well as by increased LV workload, indicating the possibility that heart failure patients with type 2 diabetes are a subgroup of patients who will receive clinical benefit by treatment with a XOR inhibitor.

5. Conclusions

The results of the present study demonstrated that XOR-mediated ROS production is increased in T2DM hearts, leading to impairment of mitochondrial respiratory chain function and ventricular dysfunction during pressure overload in diabetic hearts. Upregulation of AMPD in diabetic hearts plays a role in the increased XOR-mediated ROS production by both increasing substrate supply to XOR and inosine-mediated augmentation of XOR activity.

Funding

This study was supported by Grant-in-Aid for Scientific Research from Japan Society for the Promotion of Science (#17 K09584), Tokyo, Japan and by a grant from Sanwa Kagaku Kenkyusho, Co. Ltd., Mie, Japan.

Declaration of Competing Interest

No conflicts of interest.

Appendix A. Supplementary data

Supplementary data to this article can be found online at https://doi.org/10.1016/j.yjmcc.2021.01.002.

References

[1] T. Miki, S. Yuda, H. Kouzu, T. Miura, Diabetic cardiomyopathy: pathophysiology and clinical features, Heart Fail. Rev. 18 (2) (2013) 149–166.

[2] C.W. Yancy, M. Jessup, B. Bozkurt, J. Butler, D.E. Casey Jr., M.H. Drazner, G. C. Fonarow, S.A. Geraci, T. Horwich, J.L. Januzzi, M.R. Johnson, E.K. Kasper, W. C. Levy, F.A. Masoudi, P.E. McBride, J.J.V. McMurray, J.E. Mitchell, P.N. Peterson, B. Riegel, F. Sam, L.W. Stevenson, W.H.W. Tang, E.J. Tsai, B.L. Wilkoff, F. American College of Cardiology, G. American Heart Association Task Force on Practice, 2013 ACCF/AHA guideline for the management of heart failure: a report of the American College of Cardiology Foundation/American Heart Association task force on practice guidelines, J. Am. Coll. Cardiol. 62 (16) (2013) e147–e239.

[3] A. Rawshani, A. Rawshani, S. Franzén, N. Sattar, B. Eliasson, A.-M. Svensson, B. Zethelius, M. Miftaraj, D.K. McGuire, A. Rosengren, S. Gudbjörnsdottir, Risk factors, mortality, and cardiovascular outcomes in patients with type 2 diabetes, N. Engl. J. Med. 379 (7) (2018) 633–644.

[4] S.-A. Kim, C.-Y. Shim, J.-M. Kim, H.-J. Lee, D.-H. Choi, E.-Y. Choi, Y. Jang, N. Chung, J.-W. Ha, Impact of left ventricular longitudinal diastolic functional reserve on clinical outcome in patients with type 2 diabetes mellitus, Heart 97 (15) (2011) 1233–1238.

[5] H. Kouzu, T. Miki, M. Tanno, A. Kuno, T. Yano, T. Itoh, T. Sato, D. Sunaga, H. Murase, T. Tobisawa, M. Ogasawara, S. Ishikawa, T. Miura, Excessive degradation of adenine nucleotides by up-regulated AMP deaminase underlies afterload-induced diastolic dysfunction in the type 2 diabetic heart, J. Mol. Cell. Cardiol. 80 (2015) 136–145.

[6] Y. Tatekoshi, M. Tanno, H. Kouzu, K. Abe, T. Miki, A. Kuno, T. Yano, S. Ishikawa, W. Ohwada, T. Sato, T. Niinuma, H. Suzuki, T. Miura, Translational regulation by miR-301b upregulates AMP deaminase in diabetic hearts, J. Mol. Cell. Cardiol. 119 (2018) 138–146.

[7] Y. Amaya, K. Yamazaki, M. Sato, K. Noda, T. Nishino, T. Nishino, Proteolytic conversion of xanthine dehydrogenase from the NAD-dependent type to the O2-dependent type. Amino acid sequence of rat liver xanthine dehydrogenase and identification of the cleavage sites of the enzyme protein during irreversible conversion by trypsin, J. Biol. Chem. 265 (24) (1990) 14170–14175.

[8] E.D. Corte, F. Stirpe, The regulation of rat liver xanthine oxidase. Involvement of thiol groups in the conversion of the enzyme activity from dehydrogenase (type D) into oxidase (type O) and purification of the enzyme, Biochem. J. 126 (3) (1972) 739–745.

[9] L.C. Amado, A.P. Saliaris, S.V.Y. Raju, S. Lehrke, M. St John, J. Xie, G. Stewart, T. Fitton, K.M. Minhas, J. Brawn, J.M. Hare, Xanthine oxidase inhibition ameliorates cardiovascular dysfunction in dogs with pacing-induced heart failure, J. Mol. Cell. Cardiol. 39 (3) (2005) 531–536.

[10] H. Kögler, H. Fraser, S. McCune, R. Altschuld, E. Marbán, Disproportionate enhancement of myocardial contractility by the xanthine oxidase inhibitor oxypurinol in failing rat myocardium, Cardiovasc. Res. 59 (3) (2003) 582–592.

[11] A.V. Naumova, V.P. Chacko, R. Ouwerkerk, L. Stull, E. Marbán, R.G. Weiss, Xanthine oxidase inhibitors improve energetics and function after infarction in failing mouse hearts, Am. J. Physiol. Heart Circ. Physiol. 290 (2) (2006) H837–H843.

[12] L.B. Stull, M.K. Leppo, L. Szweda, W.D. Gao, E. Marbán, Chronic treatment with allopurinol boosts survival and cardiac contractility in murine postischemic cardiomyopathy, Circ. Res. 95 (10) (2004) 1005–1011.

[13] E.A. Jankowska, B. Ponikowska, J. Majda, R. Zymlinski, M. Trzaska, K. Reczuch, L. Borodulin-Nadzieja, W. Banasiak, P. Ponikowski, Hyperuricaemia predicts poor outcome in patients with mild to moderate chronic heart failure, Int. J. Cardiol. 115 (2) (2007) 151–155.

[14] L. Tamariz, A. Harzand, A. Palacio, S. Verma, J. Jones, J. Hare, Uric acid as a predictor of all-cause mortality in heart failure: a meta-analysis, Congest Heart Fail 17 (1) (2011) 25–30.

[15] M.G. Battelli, L. Polito, A. Bolognesi, Xanthine oxidoreductase in atherosclerosis pathogenesis: not only oxidative stress, Atherosclerosis 237 (2) (2014) 562–567.

[16] M.-C. Desco, M. Asensi, R. Márquez, J. Martínez-Valls, M. Vento, F.V. Pallardó, J. Sastre, J. Viña, Xanthine oxidase is involved in free radical production in type 1 diabetes: protection by allopurinol, Diabetes 51 (4) (2002) 1118–1124.

[17] U.R. Kuppusamy, M. Indran, P. Rokiah, Glycaemic control in relation to xanthine oxidase and antioxidant indices in Malaysian type 2 diabetes patients, Diabet. Med. 22 (10) (2005) 1343–1346.

[18] D.J. Miric, B.M. Kisic, S. Filipovic-Danic, R. Grbic, I. Dragojevic, M.B. Miric, D. Puhalo-Sladoje, Xanthine oxidase activity in type 2 diabetes mellitus patients with and without diabetic peripheral neuropathy, J. Diabetes Res. 2016 (2016), 4370490–4370490.

[19] T. Miki, T. Miura, H. Hotta, M. Tanno, T. Yano, T. Sato, Y. Terashima, A. Takada, S. Ishikawa, K. Shimamoto, Endoplasmic reticulum stress in diabetic hearts abolishes erythropoietin-induced myocardial protection by impairment of phospho-glycogen synthase kinase-3beta-mediated suppression of mitochondrial permeability transition, Diabetes 58 (12) (2009) 2863–2872.

[20] H. Murase, A. Kuno, T. Miki, M. Tanno, T. Yano, H. Kouzu, S. Ishikawa, T. Tobisawa, M. Ogasawara, K. Nishizawa, T. Miura, Inhibition of DPP-4 reduces acute mortality after myocardial infarction with restoration of autophagic response in type 2 diabetic rats, Cardiovasc. Diabetol. 14 (2015) 103.

[21] A. Takada, T. Miki, A. Kuno, H. Kouzu, D. Sunaga, T. Itoh, M. Tanno, T. Yano, T. Sato, S. Ishikawa, T. Miura, Role of ER stress in ventricular contractile dysfunction in type 2 diabetes, PLoS One 7 (6) (2012) e39893-e39893.

[22] S. Bi, T.H. Moran, Obesity in the Otsuka Long Evans Tokushima fatty rat: mechanisms and discoveries, Front Nutr 3 (2016) 21.

[23] A.S. Jaffe, J.J. Spadaro, K. Schechtman, R. Roberts, E.M. Geltman, B.E. Sobel, Increased congestive heart failure after myocardial infarction of modest extent in patients with diabetes mellitus, Am. Heart J. 108 (1) (1984) 31–37.

[24] T. Sato, H.-C. Chang, M. Bayeva, J.S. Shapiro, L. Ramos-Alonso, H. Kouzu, X. Jiang, T. Liu, S. Yar, K.T. Sawicki, C. Chen, M.T. Martínez-Pastor, D.J. Stumpo, P. T. Schumacker, P.J. Blackshear, I. Ben-Sahra, S. Puig, H. Ardehali, mRNA-binding protein tristetraprolin is essential for cardiac response to iron deficiency by regulating mitochondrial function, Proc. Natl. Acad. Sci. U. S. A. 115 (27) (2018) E6291–E6300.

[25] H. Hotta, T. Miura, T. Miki, N. Togashi, T. Maeda, S.J. Kim, M. Tanno, T. Yano, A. Kuno, T. Itoh, T. Satoh, Y. Terashima, S. Ishikawa, K. Shimamoto, Angiotensin II type 1 receptor-mediated upregulation of calcineurin activity underlies impairment of cardioprotective signaling in diabetic hearts, Circ. Res. 106 (1) (2010) 129–132.

[26] G. Luna, A.V. Dolzhenko, R.L. Mancera, Inhibitors of xanthine oxidase: scaffold diversity and structure-based drug design, ChemMedChem 14 (7) (2019) 714–743.

[27] I. Wegelin, M. Marini, G. Pane, C. Clô, Pathways of adenine nucleotide metabolism: degradation and resynthesis of IMP in ageing chicken heart, Comp. Biochem. Physiol. A Physiol. 114 (2) (1996) 99–104.

[28] F. Giacco, M. Brownlee, Oxidative stress and diabetic complications, Circ. Res. 107 (9) (2010) 1058–1070.

[29] G. Jia, A. Whaley-Connell, J.R. Sowers, Diabetic cardiomyopathy: a hyperglycaemia- and insulin-resistance-induced heart disease, Diabetologia 61 (1) (2018) 21–28.

[30] F. Stirpe, E. Dellacorte, Regulation of xanthine dehydrogenase in chick liver. Effect of starvation and of administration of purines and purine nucleotides, Biochem. J. 94 (2) (1965) 309–313.

[31] B.S. Kim, L. Serebreni, J. Fallica, O. Hamdan, L. Wang, L. Johnston, T. Kolb, M. Damarla, R. Damico, P.M. Hassoun, Cyclin-dependent kinase five mediates activation of lung xanthine oxidoreductase in response to hypoxia, PLoS One 10 (4) (2015), e0124189.

[32] A.J. Ghio, T.P. Kennedy, J. Stonehuerner, J.D. Carter, K.A. Skinner, D.A. Parks, J. R. Hoidal, Iron regulates xanthine oxidase activity in the lung, Am. J. Phys. Lung Cell. Mol. Phys. 283 (3) (2002) L563–L572.

[33] E. Martelin, R. Lapatto, K.O. Raivio, Regulation of xanthine oxidoreductase by intracellular iron, Am. J. Phys. Cell Phys. 283 (6) (2002) C1722–C1728.

[34] S. Boudina, S. Sena, B.T. O'Neill, P. Tathireddy, M.E. Young, E.D. Abel, Reduced mitochondrial oxidative capacity and increased mitochondrial uncoupling impair myocardial energetics in obesity, Circulation 112 (17) (2005) 2686–2695.

[35] S. Boudina, S. Sena, H. Theobald, X. Sheng, J.J. Wright, X.X. Hu, S. Aziz, J. I. Johnson, H. Bugger, V.G. Zaha, E.D. Abel, Mitochondrial energetics in the heart in obesity-related diabetes: direct evidence for increased uncoupled respiration and activation of uncoupling proteins, Diabetes 56 (10, 2007) 2457–2466.

[36] S. Koka, H.S. Aluri, L. Xi, E.J. Lesnefsky, R.C. Kukreja, Chronic inhibition of phosphodiesterase 5 with tadalafil attenuates mitochondrial dysfunction in type 2 diabetic hearts: potential role of NO/SIRT1/PGC-1α signaling, Am. J. Physiol. Heart Circ. Physiol. 306 (11) (2014) H1558–H1568.

[37] H.-C. Chang, R. Wu, M. Shang, T. Sato, C. Chen, J.S. Shapiro, T. Liu, A. Thakur, K. T. Sawicki, S.V.N. Prasad, H. Ardehali, Reduction in mitochondrial iron alleviates cardiac damage during injury, EMBO Mol Med 8 (3) (2016) 247–267.

[38] X. Long, M.J. Goldenthal, G.-M. Wu, J. Marín-García, Mitochondrial Ca2+ flux and respiratory enzyme activity decline are early events in cardiomyocyte response to H2O2, J. Mol. Cell. Cardiol. 37 (1) (2004) 63–70.

[39] J. Lee, S. Lee, H. Zhang, M.A. Hill, C. Zhang, Y. Park, Interaction of IL-6 and TNF-α contributes to endothelial dysfunction in type 2 diabetic mouse hearts, PLoS One 12 (11, 2017), e0187189.

[40] K.D. Pfeffer, T.P. Huecksteadt, J.R. Hoidal, Xanthine dehydrogenase and xanthine oxidase activity and gene expression in renal epithelial cells. Cytokine and steroid regulation, J. Immunol. 153 (4) (1994) 1789–1797.

[41] P. Li, K. Ogino, Y. Hoshikawa, H. Morisaki, J. Cheng, K. Toyama, T. Morisaki, K. Hashimoto, H. Ninomiya, Y. Tomikura-Shimoyama, O. Igawa, C. Shigemasa, I. Hisatome, Remote reperfusion lung injury is associated with AMP deaminase 3 activation and attenuated by inosine monophosphate, Circ. J. 71 (4) (2007) 591–596.

[42] K. Fujii, A. Kubo, K. Miyashita, M. Sato, A. Hagiwara, H. Inoue, M. Ryuzaki, M. Tamaki, T. Hishiki, N. Hayakawa, Y. Kabe, H. Itoh, M. Suematsu, Xanthine

oxidase inhibitor ameliorates postischemic renal injury in mice by promoting resynthesis of adenine nucleotides, JCI Insight 4 (22) (2019).
[43] M.M. Givertz, K.J. Anstrom, M.M. Redfield, A. Deswal, H. Haddad, J. Butler, W.H. W. Tang, M.E. Dunlap, M.M. LeWinter, D.L. Mann, G.M. Felker, C.M. O'Connor, S. R. Goldsmith, E.O. Ofili, M.T. Saltzberg, K.B. Margulies, T.P. Cappola, M. A. Konstam, M.J. Semigran, S.E. McNulty, K.L. Lee, M.R. Shah, A.F. Hernandez, N. H.F.C.R. Network, Effects of Xanthine Oxidase Inhibition in Hyperuricemic Heart Failure Patients: The Xanthine Oxidase Inhibition for Hyperuricemic Heart Failure Patients (EXACT-HF) Study, Circulation 131 (20) (2015) 1763–1771.
[44] J.M. Hare, B. Mangal, J. Brown, C. Fisher Jr., R. Freudenberger, W.S. Colucci, D. L. Mann, P. Liu, M.M. Givertz, R.P. Schwarz, O.-C. Investigators, Impact of oxypurinol in patients with symptomatic heart failure. Results of the OPT-CHF study, J. Am. Coll. Cardiol. 51 (24, 2008) 2301–2309.
[45] J. Maiuolo, F. Oppedisano, S. Gratteri, C. Muscoli, V. Mollace, Regulation of uric acid metabolism and excretion, Int. J. Cardiol. 213 (2016) 8–14.
[46] B.F. Becker, Towards the physiological function of uric acid, Free Radic. Biol. Med. 14 (6) (1993) 615–631.